



# POLITECNICO

## MILANO 1863

### Reverse Engineering of Juno Mission

#### Homework 5

Course of Space System Engineering & Operations  
Academic Year 2023-2024

#### Group 5

|                     |  |          |
|---------------------|--|----------|
| Alex Cristian Turcu | <a href="mailto:alexcristian.turcu@mail.polimi.it">alexcristian.turcu@mail.polimi.it</a>   | 10711624 |
| Chiara Poli         | <a href="mailto:chiara3.poli@mail.polimi.it">chiara3.poli@mail.polimi.it</a>               | 10731504 |
| Daniele Paternoster | <a href="mailto:daniele.paternoster@mail.polimi.it">daniele.paternoster@mail.polimi.it</a> | 10836125 |
| Marcello Pareschi   | <a href="mailto:marcello.pareschi@mail.polimi.it">marcello.pareschi@mail.polimi.it</a>     | 10723712 |
| Paolo Vanelli       | <a href="mailto:paolo.vanelli@mail.polimi.it">paolo.vanelli@mail.polimi.it</a>             | 10730510 |
| Riccardo Vidari     | <a href="mailto:riccardo.vidari@mail.polimi.it">riccardo.vidari@mail.polimi.it</a>         | 10711828 |

# Contents

|   |           |
|---|-----------|
| <b>Contents</b>   | <b>i</b>  |
| <b>Notation</b>   | <b>ii</b> |
| <b>1 Introduction of TCS</b>                                    | <b>1</b>  |
| <b>2 Analysis of thermal conditions along the mission</b>       | <b>1</b>  |
| 2.1 Thermal phases analysis . . . . .                           | 1         |
| 2.2 External heat flux analysis . . . . .                       | 1         |
| <b>3 Architecture and rationale of TCS</b>                      | <b>3</b>  |
| 3.1 Vault . . . . .   | 3         |
| 3.2 Main body . . . . .   | 3         |
| 3.3 Solar panels . . . . .                                      | 4         |
| 3.4 External hardware . . . . .                                 | 4         |
| <b>4 Reverse sizing of TCS</b>                                  | <b>5</b>  |
| 4.1 Main body . . . . .   | 5         |
| 4.2 Solar panels . . . . .                                      | 6         |
| <b>5 Appendix</b>   | <b>7</b>  |
| 5.1 Thermal limits and power usage of instrumentation . . . . . | 7         |
| <b>Bibliography</b>   | <b>8</b>  |

## Notation

|                 |  |                |   |
|-----------------|--|----------------|---|
| <b>TCS</b>      | Thermal Control System                         | <b>MLI</b>     | Multi Layer Insulation                                    |
| <b>C&amp;DH</b> | Command Data Handling                          | <b>SPM</b>     | Sun Pointing Mode   |
| <b>IMU</b>      | Inertial Measurement Unit                      | <b>EPM</b>     | Earth Pointing Mode                                       |
| <b>SRU</b>      | Stellar Reference Unit                         | <b>HGA</b>     | High Gain Antenna   |
| <b>SSS</b>      | Spinning Sun Sensor                            | <b>LILT</b>    | Low Intensity and Low Temperature                         |
| <b>MWR</b>      | Microwave Radiometer                           | <b>SOI</b>     | Sphere Of Influence                                       |
| <b>JEDI</b>     | Jupiter Energetic-particle Detector Instrument | <b>JOI</b>     | Jupiter Orbit Insertion                                   |
| <b>JADE</b>     | Jovian Auroral Distribution Experiment         | <b>EGA</b>     | Earth Gravity Assist                                      |
| <b>UVS</b>      | Ultraviolet Spectrograph                       | <b>EOM</b>     | End of the Mission  |
| <b>JIRAM</b>    | Juno Infra-Red Auroral Mapper                  | <b>IR</b>      | InfraRed  |
| <b>MAG</b>      | Magnetometer                                   | <b>ME</b>      | Main Engine   |
| <b>MOB</b>      | Magnetometer Optical Bench                     | <b>RCS</b>     | Reaction Control System                                   |
| <b>FGM</b>      | FluxGate Magnetometer                          | $q_{sun}$      | Solar heat flux [W/m <sup>2</sup> ]                       |
| <b>CCD</b>      | Charge Coupled Device                          | $q_{tot}$      | Total heat flux [W/m <sup>2</sup> ]                       |
| <b>CHU</b>      | Camera Head Unit                               | $Q_{in}$       | Internal generated heat [W]                               |
| <b>SP</b>       | Solar Panels                                   | $Q_{ht}$       | Heater power [W]  |
| <b>KaTS</b>     | Ka-band Translator                             | $Q_{lv}$       | Heat dissipated by the louvres [W]                        |
| <b>TWTA</b>     | Traveling Wave Tube Amplifier                  | $\alpha$       | Absorptivity [-]  |
| <b>SDST</b>     | Small Deep Space Transponder                   | $\varepsilon$  | Emissivity [-]  |
| <b>TP</b>       | Thermal Phase                                  | $\sigma$       | Stefan-Boltzmann constant [W/m <sup>2</sup> K]            |
| <b>LEOP</b>     | Launch and Early Orbit Phase                   | $T$            | Temperature [K]   |
| <b>IC</b>       | Inner Cruise                                   | $A_{tot}$      | Total area of equivalent sphere [m <sup>2</sup> ]         |
| <b>OC</b>       | Outer Cruise                                   | $A_c$          | Cross section area of equivalent sphere [m <sup>2</sup> ] |
| <b>DS</b>       | Deep Space                                     | $A_{sp}$       | Solar panels area [m <sup>2</sup> ]                       |
| <b>S/C</b>      | SpaceCraft                                     | $(\cdot)_{mb}$ | Main body   |
|                 |  | $(\cdot)_{sp}$ | Solar panels  |

## 1 Introduction of TCS

The Thermal Control System of Juno adopts various strategies in order to maintain the instrumentation within operative ranges of temperature. This is done through both active and passive systems, which will be analyzed in [section 3](#). First thing first, an analysis of the mission will be conducted to enlighten the thermal conditions the satellite is exposed to, which range from really hot environment nearby the Sun to extremely cold environment nearby Jupiter. A selection of the two most extreme situations will be done through a preliminary evaluation of the heat fluxes in these phases. In the light of this, the architecture of the Juno's TCS will be studied and justified through a brief rationale analysis. Finally, a reverse sizing will be carried out imposing some simplifying assumptions in order to find the temperatures on Juno and to verify the compliance with its mission.

## 2 Analysis of thermal conditions along the mission

In this section, the mission will be analyzed and divided in perspective of thermal environment encountered. During this study, the internal heat flux generated by instrumentation won't enter the reasoning. This is done because its maximum value and its variability are both contained during the mission, so it won't affect the sectioning of the TPs and the selection of the hot and the cold cases. The architecture of the S/C won't affect the reasoning and only the heat fluxes from the external environment (Sun flux, planets' albedo and IR emission) will enter this preliminary analysis. A deeper study will be conducted during the reverse sizing in [section 4](#).

### 2.1 Thermal phases analysis

Different thermal conditions have been encountered by Juno during its cruise. In previous chapters, the mission was divided into phases by different attitude and communication constraints. These phases will be now grouped by the means of thermal constraints to better analyze their evolution during the mission time.

- **TP-1:** in this first phase, which comprehends both LEOP and IC-1, the S/C is in SPM due to thermal and power requirements. In particular, since the trajectory is relatively close to the Sun, Juno has to protect the vault with the HGA (as already explained in the previous chapters). Even if TP-1 is considered a hot phase, it is not the most critical as other phases have more stringent requirements, facing longer periods closer to external heat sources (i.e. Sun and Earth).
- **TP-2:** this second phase corresponds to IC-2. Among the ICs it is the longest and the only one featuring EPM. It does not call for any particular thermal requirement, being Juno farther from both Sun and Earth. No specific attitude is required to thermally control the S/C during the different manoeuvres performed during IC-2. Neither hot nor cold phase is considered along TP-2.
- **TP-3:** the third thermal phase consists of IC-3 till the EGA, performed in SPM to protect the electronics inside the vault as the S/C passes through the perihelion of the orbit (at 0.88 AU). During TP-3, Juno was found to face the most relevant hot environment, occurring at the closest approach to the Sun. As a consequence, this condition was selected to be the hot case.
- **TP-4:** the fourth phase analyzed consists only of the EGA, from the entrance till the exit of Juno from Earth's SOI. This phase contains both a possible hot case and a possible cold case, the first due to the proximity to the planet, the latter due to the eclipse. As a consequence, this is the phase when Juno faces the highest flux excursion of the entire mission. It was found that both of the two conditions are the most extreme in terms of heat flux as the obtained results are linked with the simplified model used. As explained in [subsection 2.2](#), these conditions won't be selected as hot or cold case.
- **TP-5:** this phase is the continuation of the TP-3, except that the S/C does not encounter such high flux environment as at perihelion. It goes from the end of EGA till the end of IC-3.
- **TP-6:** this phase only includes the OC up to JOI. The S/C encounters a progressively colder environment as it is going away from the Sun. However, knowing its trajectory, Juno will face colder contexts along its mission. The transition between TP-6 and TP-7 can be seen in [Figure 2](#).
- **TP-7:** the last phase goes from the JOI till the end of the mission, including all the science orbits around Jupiter. During this period of time, the spacecraft is subject to the harsh environment of Jupiter, where it faces oscillating flux from the planet: higher nearby the perijoves and lower at the apojoves. Overall, the environment stays cold during the whole phase with a minimum when both Jupiter and Juno are around the apocentre of their respective orbits. This condition is elected as the coldest case of the entire mission.

### 2.2 External heat flux analysis

In order to find the hot and the cold cases, a simplified model of the main external heat fluxes has been carried out. All the formulas for this analysis are reported in [section 4](#). To facilitate the computation, some assumptions have been adopted:

- as previously mentioned, only the external heat fluxes have been modeled discarding the internal contribution, which is better treated in [section 4](#);
- the only contribution considered during the interplanetary phases is the Sun flux, while in proximity of the planets also albedo and IR emissions are added;
- for the hot case only TP-3 and TP-4 have been analyzed, since the other phases do not have critical condition in this sense;
- for the cold case TP-4, TP-6 and TP-7 have been analyzed, the first because of the criticality of the eclipse condition, the second because of the increasingly farther position of the S/C with respect to the Sun in an interplanetary environment, the third because Juno is orbiting Jupiter at its farthest points from the Sun;
- the analysis has been carried out from the ephemeris of the real mission instead of taking the nominal cruise;
- the  $\cos \theta$  factor in the albedo formula is assumed to be always equal to 1 as a conservative simplification, so only the distances are taken into account during the calculations.

The external heat fluxes computed by this simplified model for TP-3 ([Figure 1](#)), last year of TP-6 and whole TP-7 ([Figure 2](#)) and TP-4 ([Figure 3](#)) are shown in the plots below.

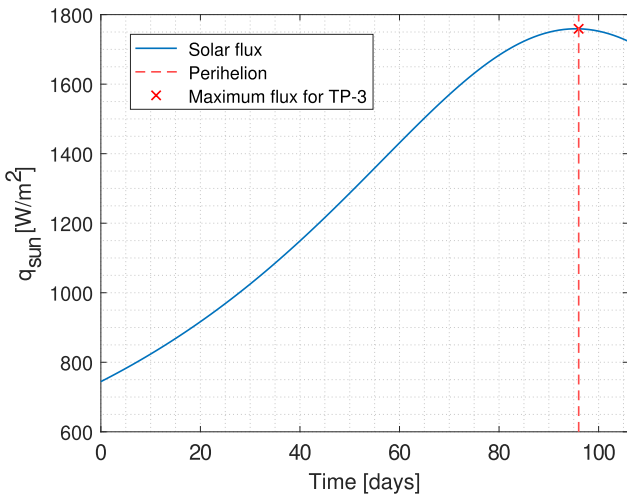


[Figure 1](#): Flux analysis of TP-3

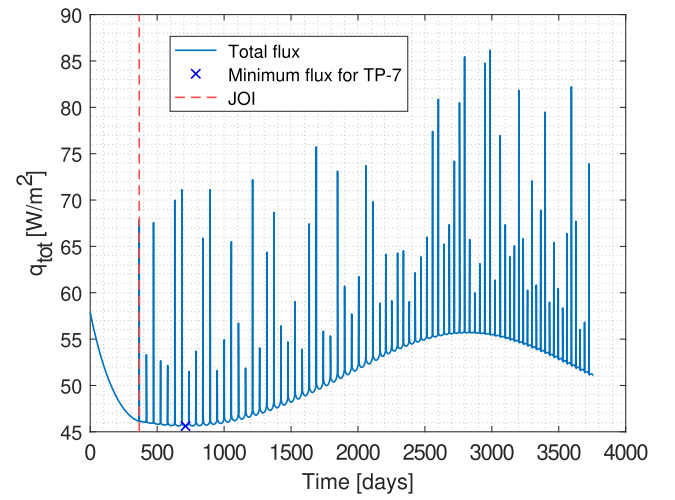


[Figure 2](#): Flux analysis of end of TP-6 and whole TP-7

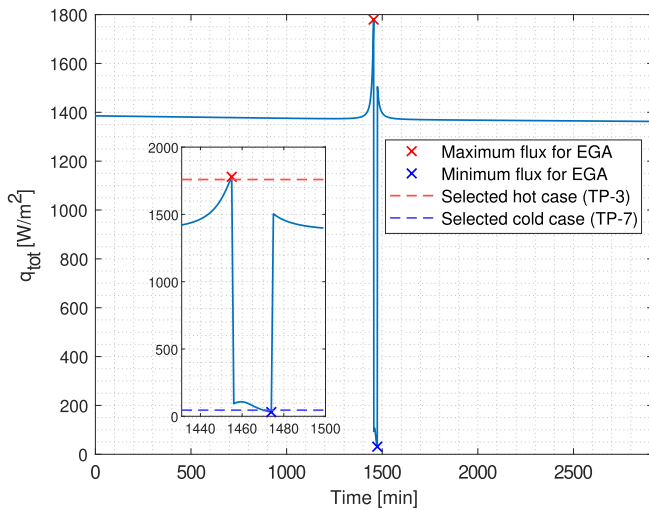


[Figure 3](#): Flux analysis of TP-4 (EGA phase)

| Phase          | $q_{tot}$ [W/m <sup>2</sup> ] |
|----------------|-------------------------------|
| TP-4 hot case  | 1779.32                       |
| TP-3 hot case  | 1759.23                       |
| TP-4 cold case | 31.13                         |
| TP-7 cold case | 45.62                         |

[Table 1](#): Summary of considered hot and cold cases

It is worth noting that the flux derived from both planets' albedo contribution is greatly overestimated due to the simplification discussed before. Despite TP-4 presents both the hottest and the coldest points of the whole mission, the time spent by Juno in these regions is limited. As can be noticed in [Figure 3](#), the S/C spends only around half a minute in an environment characterized by a heat flux above the one of the hot case (TP-3) and spends around four minutes in an environment where the heat flux is below the one of the cold case (TP-7). Moreover, as can be also seen in [Table 1](#), the cases are very close to each other. For this reason, the choice is to not consider EGA's peaks as hot and cold cases, also because in reality Juno has to overcome a transient before reaching extreme temperatures.

The passage from perihelion during TP-3 is hence selected to be the most significant hot environment. On the other side, the most relevant cold case was found to be a few orbits after JOI, around the farthest position of Juno from both Sun and Jupiter, where both solar flux and the planet's contribution are at their lowest. Particularly, in Figure 2 oscillations with two different frequencies can be observed: the long period one is related to Jupiter's lightly elliptical orbit around the Sun, the short term oscillation, with its peaks, is related to Juno's highly elliptical orbit around Jupiter. The chosen resolution for the ephemeris determines the non-uniformity of the observed peaks.

### 3 Architecture and rationale of TCS

The TCS of Juno must tackle a wide range of thermal environments, as discussed in section 1. The cold case however is the most critical condition for the S/C, so TCS is mainly designed on this situation: the vault, the main body and the external hardware are all thermally insulated and decoupled. Heaters are also present on each individual section/sensor. This guarantees flexibility in order to ensure the operating temperature for each component. Four main thermal zones were identified on the basis of the different thermal requirements of the components and their positioning.

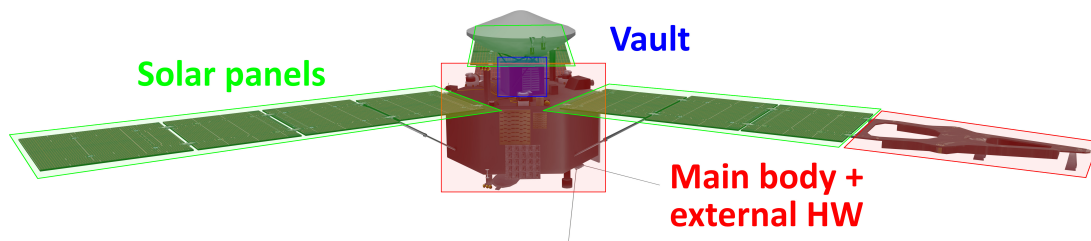


Figure 4: Thermal subdivision of Juno

#### 3.1 Vault

All the main electronic hardware is contained inside the vault. The size of this box is  $0.8 \text{ m} \times 0.8 \text{ m} \times 0.7 \text{ m}$ . The lower surface is attached to the main body while the top surface is linked to the HGA, lateral surfaces points outwards and mainly to deep space. The walls are made of 1 cm thick titanium walls<sup>[1]</sup>. This metal has a low conductivity value ( $\approx 6.7 \div 7.4 \text{ W/mK}$ ) which is a positive feature for the cold case at Jupiter. Also, major heat generation happens during science orbits since all the instrument electronics is powered on. In addition, the low external thermal flux during science imposes additional requirements in relation to the optical properties of the lateral vault surfaces. Tantalum MLI blankets were used in order to ensure both low emissivity and absorptivity ( $\varepsilon \approx 0.01 \div 0.035$ <sup>[2]</sup>). However, during the phases in which the thermal flux is at its highest (TP-3), the vault shall be able to dissipate enough power. This is in contrast with the above mentioned design choices. To ensure compatible thermal environment in the vault, three louvres were applied on its external lateral surfaces in order to point deep space and have an efficient IR emission. The dimension of a single louvre is  $0.53 \text{ m} \times 0.40 \text{ m}$ , two of them are placed vertically while one of them is placed horizontally. The motivation for this choice is relative to the internal configuration of the electronics. The opening of the louvre's shutters raises the emissivity value from 0.14 to 0.74, enabling higher out-going radiative heat flux.<sup>[3]</sup> The justification for this passive and low complexity solution was mainly due to the fact that the hot case scenario was encountered only during a restricted time of the overall mission. Moreover, the louvre technology effectiveness was tested and ensured by previous interplanetary mission such as Rosetta and New Horizons. However, most of the radiation coming from the Sun was shielded by the HGA which protected the vault. The Germanium coated Kapton used to cover the antenna dish has an operating range temperature of  $-200 \text{ }^{\circ}\text{C} \div +200 \text{ }^{\circ}\text{C}$ , while its absorptivity and emissivity values are  $\alpha = 0.568$  and  $\varepsilon = 0.72$  respectively<sup>[4]</sup>. The HGA will heat up and exchange radiative heat with the lower vault, hence the necessity to dissipate heat also from the electronic vault with louvres. The electronics contained in the vault are tightly packed to reduce the effects of internal reflection of high energy particles that can still penetrate the walls. From a thermal viewpoint this means that the generated heat is better retained and the internal temperature of the hardware is fairly uniform.

#### 3.2 Main body

The main body is the hexagonal prism that contains most of the propulsion subsystem hardware (propellant and pressurizer tanks, feeding lines and ME). Two payload sensors are also present inside, namely UVS and JunoCam. All of these elements require separated strategies to manage the temperatures.

The six spherical propellant tanks (two of oxidizer and four of fuel) are arranged into six bays that corresponds to the equally distributed volumes of the hexagonal prism. Hence, each compartment contains just one tank and it is thermally uncoupled from the others in order to guarantee a better independent and redundant thermal management. To ensure this uncoupling, high reflectance blankets are used over the tank surface. Nominally, aluminized polyester film is used ( $\alpha/\varepsilon \approx 3.5$ ). This material minimizes heat flow to and from the S/C, it is generally



used for temperature ranges from  $-250\text{ }^{\circ}\text{C}$  to  $+120\text{ }^{\circ}\text{C}$  and has been successfully used on previous missions<sup>[5]</sup>. The tanks are made of titanium which has low thermal conductivity. The honeycomb composite lateral walls of each bay are also covered with high reflectance coating to ensure radiative insulation. In addition, heaters are present into the propellant tanks, helium tanks and also feeding lines.<sup>[6]</sup> Other thermal considerations on the internal main body refers to the operations of the main engine which is mainly inside the central body. In that moments high thermal flux must be handled by the internal structure which must be thermally decoupled both radiatively and conductively.

### 3.3 Solar panels

Three solar arrays are present on the spacecraft to provide electricity throughout the different phases of the mission. They are connected to the main body through hinges and struts. To guarantee the correct pointing towards the Sun, stiffness was required to avoid deformation during the spin. This was obtained using carbon fiber supports on which all the cells are placed. The configuration allows each panel to have a clear view of both Sun and DS: dissipation of heat occurs from both front and back faces as the view factor between panels and Juno's main body is close to 0. Given the described geometry, solar arrays can be modeled as thermally decoupled from the rest of the S/C.

To ensure the proper functioning in drastically diverse environments, solar panels were designed to withstand a wide range of temperatures, going from the predicted  $+100\text{ }^{\circ}\text{C}$  of the perihelium to the  $-140\text{ }^{\circ}\text{C}$  around Jupiter<sup>[7]</sup>. Moreover, the whole spacecraft has to survive to radiations up to  $10^{15}\text{ MeV}$  so a custom made CMG coverglass with coating was employed. Every cell of the panels is thus covered on the front side with a  $304\text{ }\mu\text{m}$ , 14.3 mil fused silica equivalent<sup>[7]</sup>, anti-reflective coating and Indium Tin Oxide, the first to improve performance in a LILT environment, the second to mitigate surface charge buildup<sup>[7]</sup>. The rear side shielding of each panel's substrate is shielded with a 30 mils fused silica equivalent of Kapton and Germanium. In order to guarantee the correct amount of electricity during science operations, around 440 W at JOI and 400 W at EOM, the arrays are drastically oversized at any distance below 5.4 AU: at 1 AU 14 kW are produced. During the ICs and OC, more electricity than needed is generated but left on the panels in the form of heat that must be dissipated from both front and back faces. To do so, different kinds of coatings are used: values for emissivity vary from 0.84 to 0.88 for Black Kapton on the back side and from 0.66 to 0.88 for the Kapton between cells and the carbon fiber support on the front side. Coverglass on the front side is transparent to the incoming radiation, but it is able to emit towards the DS with an emissivity ranging from 0.73 to 0.82. All the intervals for the reported coefficients are related to hot and cold case<sup>[7]</sup>.

### 3.4 External hardware

The external hardware thermal zone comprehends all the remaining payload sensors (JADE, JEDI, Waves, MWR, MAG, JIRAM), SRUs, SSSes, batteries, antennas and RCS. Waves and JIRAM are located on the aft deck which can be thought as a cold side since it points deep space. All this hardware is installed either on the main body or on the edge of the solar arrays, hence the visual coupling of main body and external hardware thermal zones in [Figure 4](#). JIRAM does not have a minimum temperature range for its sensor, the maximum operating temperature is 95 K in order to have useful scientific data.<sup>[8]</sup> Waves sensing unit is composed of the antenna and the pre-amplifier unit which is thermally coated. Conversely to the sensors on the aft deck<sup>[9]</sup>, JADE and JEDI have minimum operative temperature so they are located on the surface that is in visibility of the Sun (top deck). Moreover, the 4 sensors of JADE and the sensor of JEDI are not directly shielded by the HGA.<sup>[10][11]</sup> MWR antennas are positioned on two of the six lateral surfaces of the main body.<sup>[12]</sup> No stringent requirements are presented for this hardware. During Juno operative life at Jupiter these sensors will face the planet's surface, hence the incoming radiation: albedo and infrared. MAG payload positioning is much more critical under the thermal point of view. The payload is made of two MOBs, each one of them contains the FGM and two CHUs. The two boards are for redundancy. For mechanical and thermal stability requirements, the two MOBs, made of Carbon Silicon Carbide, are linked to the MAG boom, that is composed by aluminum honeycomb between two carbon sheets. To ensure thermal decoupling from the structure, the joints between the magnetic boom and MOBs are made of titanium. Regarding the sensors, both the FGMs and CHUs are located on the side that is pointing deep space. The FGM sensor is enclosed individually within a multilayer thermal blanket and thermally stabilized at all times by a non-magnetic resistive heater driven by an alternating current, which keep the FGM operating temperature close to  $0\text{ }^{\circ}\text{C}$ . The temperature gradient between the FGM unit and the MOB is of  $80\text{ }^{\circ}\text{C}$ , to reduce the thermal strains on the joints between these two units are made of three titanium joints. This has a double effect: reduce the rotation induced by the gradient and reduce the thermal coupling due to the low conductivity and smaller area of contact. Conversely, the CHUs run at much lower temperature ( $-54\text{ }^{\circ}\text{C}$ ) and thermal gradient is much lower. Their body is made of titanium, they are thermally conditioned with resistive heaters and enclosed into a MLI blanket.

The SRUs (two for redundancy) are located on the top deck, so they receive solar flux while S/C is pointing Earth or Sun. Their hardware is sensible to radiation so the internal components are heavily shielded with tungsten and titanium, the first is thermally conductive while the second is not. Moreover, copper is used as a heat sink to transport thermal energy on the CCD, which is the sensible part of the apparatus.<sup>[13]</sup>

RCSs contain also thermal sensible materials, such as the catalytic bed Shell-405, which cannot withstand very cold

environment and it is susceptible to thermal cycles. As a consequence, each set of the three thrusters is heavily shielded and heaters are placed to maintain a minimum temperature.<sup>[14]</sup> Most of the external hardware is covered with MLI which guarantees radiative decoupling with low values of emissivity and absorptivity. Moreover, these layers serve as additional protection to the high energy particles radiation of the Jupiter environment.

## 4 Reverse sizing of TCS

The reverse sizing of Juno's TCS focuses independently on the main body and the solar arrays, as they are thermally isolated from each other (subsection 3.3). For all analyses only the solar heat flux was considered, as all other fluxes have negligible influence, while the deep space temperature is considered to be 0 K for ease of calculation.

### 4.1 Main body

A first approximate model for the main body consists in a mononodal analysis of an equivalent sphere of the S/C. This sphere has the same area as the exterior of the hexagonal body, radiation vault and HGA combined, for a total of  $A_{tot} = 34.78 \text{ m}^2$ . The internal generated heat  $Q_{in}$  has been recovered from Table 6. Its value is reported in Table 2 together with the solar heat flux for both cases. From the same Table 6 the most stringent operating temperature range was also recovered, ranging from  $-10^\circ \text{C}$  to  $+30^\circ \text{C}$ .

|                  | $q_{sun} [\text{W/m}^2]$ | $Q_{in} [\text{W}]$ |
|------------------|--------------------------|---------------------|
| <b>Hot case</b>  | 1759.23                  | 133.48              |
| <b>Cold case</b> | 45.62                    | 297.01              |

Table 2: Mononodal analysis solar heat flux and internal heat

Considering now that only the cross section of the sphere is illuminated by the Sun while the whole surface radiates into deep space, the following equation can be recovered by imposing heat equilibrium.

$$\alpha A_c q_{sun} + Q_{in} = \sigma \varepsilon A_{tot} T_{mb}^4 \quad (1)$$

This equation can be rewritten to obtain  $\alpha$  as a linear function of  $\varepsilon$ , by fixing all other parameters.

$$\alpha = \frac{\sigma A_{tot} T_{mb}^4}{A_c q_{sun}} \varepsilon - \frac{Q_{in}}{A_c q_{sun}} \quad (2)$$

Substituting the extremes of the temperature range for both thermal cases defines two couples of lines in the  $\varepsilon - \alpha$  plane. Each pair encompasses a region of plane in which the S/C can operate without any thermal control as seen in Figure 5. Their intersection identifies all  $(\varepsilon, \alpha)$  couples that allow safe operation in both cases.

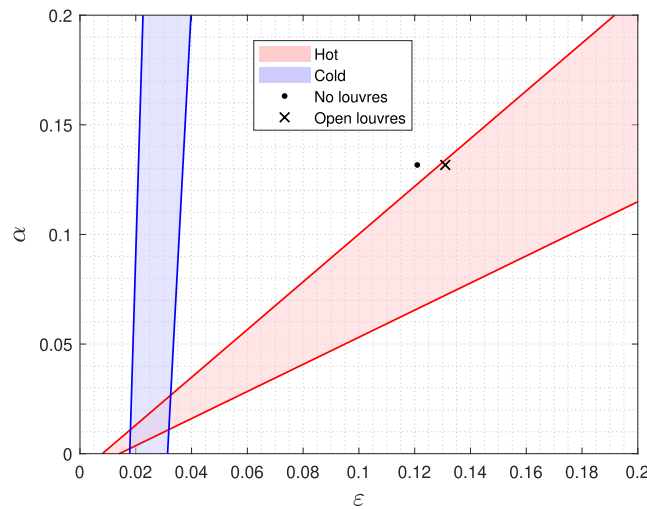


Figure 5: Admissible  $(\varepsilon, \alpha)$  couples

The black dot identifies the specific  $\varepsilon_{mb}$  and  $\alpha_{mb}$  values of the S/C (0.121 and 0.132 respectively), computed as the weighted average of the optical characteristics of the various external surfaces, highlighted in section 3, without considering any thermal control hardware. It clearly does not fall into any of the two previously identified regions, meaning that in this model Juno requires both radiators/louvres and heaters to function properly. In fact it's possible



to calculate the S/C temperature from Equation 1 imposing all previously defined parameters in both cases. The results are reported in Table 3 and, as expected, they are outside the valid range previously identified.

| $T_{mb}^{(hot)} [^{\circ}\text{C}]$ | $T_{mb}^{(cold)} [^{\circ}\text{C}]$ |
|-------------------------------------|--------------------------------------|
| 34.91                               | -77.53                               |

Table 3: Main body temperatures

For both the hot and cold case, then, the minimum heat that needs to be exchanged to keep the temperature inside its range can be computed ( $Q$  is positive if heat is entering the S/C):

$$Q_{ht} = \sigma \varepsilon_{mb} A_{tot} T_{min}^4 - \alpha_{mb} A_c q_{sun}^{(cold)} - Q_{in}^{(cold)} = 794.5 \text{ W} \quad (3)$$

$$Q_{lv} = \sigma \varepsilon_{mb} A_{tot} T_{max}^4 - \alpha_{mb} A_c q_{sun}^{(hot)} - Q_{in}^{(hot)} = -133.8 \text{ W} \quad (4)$$

Where  $Q_{ht}$  is the heater power required to keep Juno's main body at the minimum temperature of  $-10^{\circ}\text{C}$  during the cold case and  $Q_{lv}$  is the heat that needs to be removed to maintain the temperature at  $+30^{\circ}\text{C}$  in the hot case. The latter can be easily handled by the louvres present on the S/C as can be seen by the position of the black "x" in Figure 5, which is inside the hot case viable region.  $Q_{ht}$ , instead, is completely unrealistic, especially considering that the solar arrays only produce  $\approx 420 \text{ W}$  at Jupiter<sup>[7]</sup>. This is caused by the fact that Juno's main body consists of various sections with totally different thermal characteristics and requirements which can't really be lumped all together in a single spherical node model. A multinodal approach that considers both the complex geometry of Juno and the optical properties of each surface independently would yield more realistic conclusions. Furthermore, the results are also in contrast with the cold-biased design of the S/C, where a larger  $Q_{lv}$  and a smaller  $Q_{ht}$  (in magnitude) would be expected. This is due to the fact that only radiative heat transfer was considered in the model, while neglecting completely the considerable external insulation.

## 4.2 Solar panels

For the solar panels a mononodal analysis was also employed, but in this case the considered geometry is a flat plate with the total area of the solar panels  $A_{sp} = 60 \text{ m}^2$ . In reality the three arrays are physically separated from each other, but there are no reasons to believe that they will exhibit different thermal behaviors, so they were studied as a single entity. The panels have high absorptivity on the side which points the Sun. This side also points deep space, hence it emits in the infrared. Regarding the back of the solar arrays, the surface only emits in the infrared to deep space. The mathematical modelling is described by the following formula:

$$\alpha_{sp} A_{sp} q_{sun} - Q_{in} = \sigma \varepsilon_{sp} 2 A_{sp} T_{sp}^4 \quad (5)$$

Where  $\alpha_{sp}$  is the absorptivity of the front surface of the solar array, that is pointing the Sun.  $Q_{in}$  is the requested power from all the other hardware of the S/C (without considering heaters), which depends on the mission phase.  $\varepsilon_{sp}$  is the mean emissivity of the front and back surfaces of the solar array, as both irradiate to deep space, weighted on the area. Since they are equal, it turns out to be just the arithmetic mean. By inverting Equation 5:

$$T_{sp} = \sqrt[4]{\frac{\alpha_{sp} A_{sp} q_{sun}}{\sigma \varepsilon_{sp} 2 A_{sp}} - \frac{Q_{in}}{\sigma \varepsilon_{sp} 2 A_{sp}}} \quad (6)$$

The known values are the following

| $\alpha_{sp} [-]$ | $\varepsilon_{sp} [-]$ | $A_{sp} [\text{m}^2]$ | $Q_{in}^{(hot)} [\text{W}]$ | $Q_{in}^{(cold)} [\text{W}]$ | $q_{sun}^{(hot)} [\text{W}/\text{m}^2]$ | $q_{sun}^{(cold)} [\text{W}/\text{m}^2]$ |
|-------------------|------------------------|-----------------------|-----------------------------|------------------------------|---|--|
| 0.92              | 0.825                  | 60                    | 133.48                      | 297.01                       | 1759.23                                 | 45.62                                    |

Table 4: Input data for solar panels

The temperatures obtained in the two cases are expressed in Table 5. Both values are compliant with the specifics of the solar panels given in Table 6, so no additional radiators or heaters are needed. These results are also inline with a thermal simulation of the panels performed by NASA itself.<sup>[7]</sup>

| $T_{sp}^{(hot)} [^{\circ}\text{C}]$ | $T_{sp}^{(cold)} [^{\circ}\text{C}]$ |
|-------------------------------------|--------------------------------------|
| 89.39                               | -132.11                              |

Table 5: Calculated solar panels temperatures

## 5 Appendix

### 5.1 Thermal limits and power usage of instrumentation

In the following table values for temperature range, power consumption of the different instruments are reported, as well as their respective position.

| Instrumentation                                  | Specific element | Temperature range [°C] | Dissipated power [W] | Position  |
|--|------------------|------------------------|----------------------|-----------|
| <b>C&amp;DH</b> <sup>[15][16]</sup>              | -                | -55 to +70             | 2 × 12               | Vault     |
| <b>Tanks &amp; feeding lines</b> <sup>[14]</sup> | -                | +10 to +35             | -                    | Main body |
| <b>Engines</b> <sup>[14][17]</sup>               | ME               | -53 to +65             | -                    | Main body |
|  | RCS              | > 0                    | 12 × 5.39            | External  |
| <b>IMU</b> <sup>[18]</sup>                       | -                | -10 to +60             | 2 × 43               | Vault     |
| <b>SRU</b> <sup>[19]</sup>                       | Electronics      | N/A                    | 2 × 6.3              | Vault     |
|  | Optical head     | -30 to + 60            | 2 × 3.7              | External  |
| <b>JADE</b> <sup>[10]</sup>                      | E sensors        | -25 to +40             | 3 × 0.67             | External  |
|  | I sensors        | -25 to +40             | 3.8                  | External  |
|  | Electronics      | -10 to +45             | 18.1                 | Vault     |
| <b>JEDI</b> <sup>[11]</sup>                      | Sensors          | N/A                    | 3 × 3.1              | External  |
|  | Electronics      | N/A                    | 1.53                 | Vault     |
| <b>KaTs</b> <sup>[20]</sup>                      | -                | -40 to +65             | 40                   | Vault     |
| <b>TWTA</b> <sup>[21]</sup>                      | -                | N/A                    | 2 × 31               | Vault     |
| <b>SDST</b> <sup>[22]</sup>                      | X/X              | -40 to +60             | 15.8                 | Vault     |
|  | X/X & X/Ka       | -40 to +60             | 19.5                 | Vault     |
| <b>Batteries</b> <sup>[23]</sup>                 | -                | -20 to +40             | -                    | External  |
| <b>MWR</b> <sup>[12]</sup>                       | Sensors          | N/A                    | -                    | External  |
|  | Electronics      | -15 to +30             | 32.6                 | Vault     |
| <b>Waves</b> <sup>[9]</sup>                      | Sensors          | N/A                    | -                    | External  |
|  | Electronics      | -35 to +75             | 6                    | Vault     |
| <b>UVS</b> <sup>[24]</sup>                       | Sensors          | N/A                    | 2.5                  | Main body |
|  | Electronics      | -20 to +40             | 7.3                  | Vault     |
| <b>JunoCam</b> <sup>[25]</sup>                   | -                | -30 to +75             | 5.9                  | Main body |
| <b>JIRAM</b> <sup>[8]</sup>                      | -                | < -173 <sup>I</sup>    | 15                   | External  |
| <b>MAG</b> <sup>[13]</sup>                       | Sensors          | -35 to +75             | N/A                  | External  |
|  | Electronics      | -40 to +80             | N/A                  | Vault     |
| <b>SP</b> <sup>[7]</sup>                         | -                | -140 to +100           | -                    | External  |

Table 6: Instruments thermal limits and power usage

<sup>I</sup> This value only refers to the operational range of temperatures, no limits were found for non operational conditions.

## Bibliography

- [1] Installing Juno's radiation vault. *Radiation vault characteristics*. Website. Site: <https://www.nasa.gov/image-article/installing-junos-radiation-vault/>. 2024.
- [2] Robert F. Coker. "Thermal Design and Analysis of Europa Clipper's Radio Frequency Module". In: (2019).
- [3] Sierra Nevada Corporation. *Passive thermal louvers*. 2017.
- [4] A. Carmel Mary Esther et al. "A study on degradation of germanium coating on Kapton used for spacecraft sunshield application". In: (2015).
- [5] Site: <https://www.dunmore.com/products/aluminized-polyester-film.html>.
- [6] Jeff Lewis. "Juno Spacecraft Operations Lessons Learned for Early Cruise Mission Phases". In: (2014).
- [7] William McAlpine et al. "JUNO Photovoltaic Power at Jupiter". In: (2012).
- [8] R.Noschese et al. "JIRAM Standard Product, Data Record and Archive Volume, Software Interface Specification". In: (2013).
- [9] B.T. Mokrzycki et al. "The Juno Waves Investigation". In: (2017).
- [10] D.J. McComas et al. "The Jovian Auroral Distributions Experiment (JADE) on the Juno Mission to Jupiter". In: (2012).
- [11] S.E. Jaskulek et al. "The Jupiter Energetic Particle Detector Instrument (JEDI) Investigation for the Juno Mission". In: (2013).
- [12] M.A. Janssen et al. "MWR: Microwave Radiometer for the Juno Mission to Jupiter". In: (2016).
- [13] R. Schnurr et al. "The Juno Magnetic Field Investigation". In: (2016).
- [14] Nammo. *Leros 1b engine*. Journal of Geophysical Research: Planet. Site: <https://www.nammo.com/wp-content/uploads/2021/03/2021-Nammo-Westcott-Liquid-Engine-LEROS1B.pdf>.
- [15] BAE Systems. *Rad750 experience: The challenge of SEE hardening a high performance commercial processor*. 2002.
- [16] BAE Systems. *RAD750 3U CompactPCI single-board computer*.
- [17] *MR-111C datasheet*. Site: <http://www.astronautix.com/m/mr-111.html>.
- [18] Northrop Grumman. *Scalable SIRU™ Family*. Site: <https://cdn.northropgrumman.com/-/media/wp-content/uploads/pdf/Scalable-SIRU-family-of-products-brochure.pdf?rev=57f1ba8ddcb44783b9e97f979b6e45d9>.
- [19] Leonardo S.p.A. *AUTONOMOUS STAR TRACKERS*. Site: [https://space.leonardo.com/documents/16277711/19573187/Copia\\_di\\_A\\_STR\\_Autonomous\\_Star\\_Trackers\\_LQ\\_mm07786\\_.pdf?t=1538987562062](https://space.leonardo.com/documents/16277711/19573187/Copia_di_A_STR_Autonomous_Star_Trackers_LQ_mm07786_.pdf?t=1538987562062).
- [20] S. Ciarcia et al. "MORE AND JUNO KA-BAND TRANSPONDER DESIGN, PERFORMANCE, QUALIFICATION AND IN-FLIGHT VALIDATION". In: (2013).
- [21] Anthony P. Mittskus et al. "Juno Telecommunications". In: (2012).
- [22] General Dynamics. *Small Deep-Space Transponder (SDST)*. 2019.
- [23] Eaglepicher technologies. *Proven battery technology utilizing high energy, long-cycle life, low weight and small volume lithium-ion cells*. 2022.
- [24] G. Randall Gladstone et al. "The Ultraviolet Spectrograph on NASA's Juno Mission". In: (2013).
- [25] C.J. Hansen et al. "Junocam: Juno's Outreach Camera". In: (2013).